E_1, E_2, and E_0' transitions and pressure dependence in ordered $Ga_{0.5}In_{0.5}P$

Su-Huai Wei, Alberto Franceschetti, and Alex Zunger
National Renewable Energy Laboratory, Golden, Colorado 80401
(Received 8 November 1994)

We investigated theoretically the ordering-induced change of the E_1, E_2, and E_0' transitions in $Ga_{0.5}In_{0.5}P$ using symmetry arguments and first-principles band-structure calculations. We show that upon (111) superlattice ordering these transitions are altered dramatically—some states shift up in energy, some shift down, and new "ordering-induced" transitions, absent in the disordered phase, now become allowed. Experimental observation of these changes could serve as new fingerprints of ordering. We have also studied the pressure dependence of the energies of the X_{1c} and L_{1c} derived states in the ordered superlattice. The recent experimental observation of the "X_{1c}-like" state at higher pressure is identified as a mixture of the folded L_{1c} and X_{1c} states. A microscopic explanation is given.

I. INTRODUCTION

Spontaneous CuPt ordering of many III-V alloys, including $Ga_{0.5}In_{0.5}P$, has been widely observed in vapor phase growth on (001) substrates.[1] This type of ordering is known[2–9] to cause a splitting at the valence-band maximum and a lowering of the fundamental band gap (the E_0 transition) relative to the random alloy. Extensive theoretical[2–5] and experimental [6–9] work has been carried out to study the ordering-induced effects on the lowest direct E_0 transition at Γ. In this work we focus on ordering-induced changes in the higher-energy transitions E_1, E_2, and E_0' in $Ga_{0.5}In_{0.5}P$. In the disordered zinc-blende III-V semiconductors alloys (see below), the E_1 transition[10] ($\Lambda_{4v,5v} \leftrightarrow \Lambda_{6c}$) comes from pairs of states along the Λ line in a region near L, the E_2 transition[10] ($X_{7v} \leftrightarrow X_{6c}$) comes from pairs of states in a region close to X, and the E_0' transition[10] ($\Gamma_{8v} \leftrightarrow \Gamma_{7c}$) comes from pairs of states in a region close to Γ. For disordered $Ga_{0.5}In_{0.5}P$, the E_1, E_2, and E_0' transitions are measured at about[10] 3.3, 5.1, and 4.8 eV, respectively. In this work, we follow the evolution of these states from the disordered alloy to the ordered structures. We first use symmetry consideration and then apply first-principles band theory, thus obtaining quantitative evaluations. We show that, upon ordering, these transitions are altered dramatically—some states shift up in energy, some shift down, and new ordering-induced transitions, absent in the disordered phase, now become allowed. Experimental observation of these changes could serve as new fingerprints of ordering. Our results compare well with recent experimental data.[11,12] We have also studied the positions of the X_{1c}- and L_{1c}-derived states in the ordered superlattice and found that they are unchanged relative to the disordered alloy at zero pressure. The experimentally observed "X_{1c}-like" state at higher pressure[13] is identified here as a mixture of the folded L_{1c} and X_{1c} states.

II. SYMMETRY CONSIDERATION

When a zinc-blende disordered alloy forms an ordered superlattice, its band structure folds into the smaller superlattice Brillouin zone. Those folded states that have the same superlattice symmetry can couple to each other by the difference between the superlattice and disordered alloy potential. This coupling potential has both a chemical piece (given by the difference in atomic potentials of the undistorted systems) and a structural piece (given by displacements caused by the atomic size difference). This coupling can lead to an energy-level shift and to splitting of those states that were degenerate in the (higher-symmetry) zinc-blende alloy. For CuPt superlattice ordering (i.e., monolayer alternation along [111]), the unit cell of the ordered structure is twice as large as the zinc-blende cell, so its Brillouin zone (Fig. 1) is half that of the zinc-blende zone. Consequently, two zinc-blende **k** points fold into a single **k** point in the CuPt Brillouin zone. Denoting superlattice states by an overbar, and showing in parentheses the zinc-blende state from which they evolve (using single space-group notations), we now distinguish the following folded states in a (111)-ordered superlattice.

(a) Along the [111] ordering direction the Λ line between Γ and $L_{111}/2$ and the line between L_{111} and $L_{111}/2$ both fold into the same superlattice $\bar{\Gamma}$-$\bar{Z}$ line, denoted as $\bar{\alpha}$ in Fig. 1. The symmetry at the $\bar{\Gamma}(\Gamma)$ point is reduced from T_d in zinc-blende alloy to C_{3v} in the CuPt superlattice, hence the threefold-degenerate (neglecting spin degeneracy) Γ_{15} states split into twofold-degenerate $\bar{\Gamma}_3$ and single $\bar{\Gamma}_1$ states. The symmetry of the other points on this line (C_{3v}, the same as the $\bar{\Gamma}$ point) is

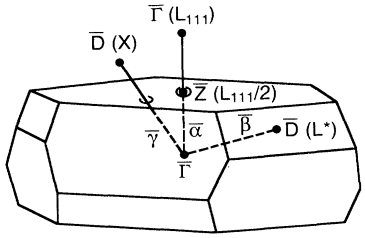

FIG. 1. Brillouin zone of the CuPt-ordered superlattice. High-symmetry superlattice points (solid dots) are denoted by an overbar. The corresponding zinc-blende points are given in parentheses.

not reduced, so no further splitting occurs.

(b) The three other zinc-blende Λ lines connecting Γ with L^*, where L^* denotes $\pi/a(\bar{1}11)$, $\pi/a(1\bar{1}1)$, and $\pi/a(11\bar{1})$ points, all fold into three symmetry-equivalent superlattice $\bar{\Gamma}$-$\bar{D}$ lines, denoted as $\bar{\beta}$ in Fig. 1. The C_{3v} symmetry along this zinc-blende Λ line is reduced in the superlattice to C_s, hence the doubly degenerate Λ_3 state splits into $\bar{\beta}_1$ and $\bar{\beta}_2$, while the L_3 state splits into $\bar{D}_1$ and $\bar{D}_2$ states. The zinc-blende $L_{111}-X$ line also folds into the same $\bar{\beta}$ line. Thus the doubly degenerate X_5 state also splits into $\bar{D}_1$ and $\bar{D}_2$ states.

(c) The three zinc-blende Δ lines connecting Γ with X fold into other three symmetry-equivalent superlattice $\bar{\Gamma}$-$\bar{D}$ lines, denoted as $\bar{\gamma}$ in Fig. 1. The C_{4v} symmetry along this zinc-blende Δ line is reduced in the superlattice to C_s, hence the doubly degenerate Δ_5 state splits into $\bar{\gamma}_1$ and $\bar{\gamma}_2$ states. The zinc-blende L_{111}-L^* lines also fold into the $\bar{\gamma}$ lines.

With these definitions of folding relations, it is now possible to draw an analogy between the E_1, E_2, and E_0' transitions in the zinc-blende disordered alloy and in the CuPt-ordered superlattice, namely

$$E_1(\Lambda_{4v,5v}\leftrightarrow\Lambda_{6c})\rightarrow E_1^a[\bar{\beta}_{3v}(\Lambda_{3v})\leftrightarrow\bar{\beta}_{3c}(\Lambda_{1c})]$$

$$E_1^b[\bar{\beta}_{4v}(\Lambda_{3v})\leftrightarrow\bar{\beta}_{3c}(\Lambda_{1c})]$$

$$E_1^c[\bar{\alpha}_{4v,5v}(\Lambda_{3v})\leftrightarrow\bar{\alpha}_{6c}(\Lambda_{1c})]\ , \quad (1)$$

$$E_2(X_{7v}\leftrightarrow X_{6c})\rightarrow E_2^a[\bar{\gamma}_{3v}(X_{5v})\leftrightarrow\bar{\gamma}_{3c}(X_{1c})]$$

$$E_2^b[\bar{\gamma}_{4v}(X_{5v})\leftrightarrow\bar{\gamma}_{3c}(X_{1c})]\ , \quad (2)$$

$$E_0'(\Gamma_{8v}\leftrightarrow\Gamma_{7c})\rightarrow E_0'^a[\bar{\Gamma}_{4v,5v}(\Gamma_{15v})\leftrightarrow\bar{\Gamma}_{6c}(\Gamma_{15c})]$$

$$E_0'^b[\bar{\Gamma}_{6v}(\Gamma_{15v})\leftrightarrow\bar{\Gamma}_{6c}(\Gamma_{15c})]\ . \quad (3)$$

We see that the E_1 alloy transition splits into at least three transitions: two that evolve from the $\bar{\beta}$-folded Λ_{3v}-split states, and one that corresponds to the $\bar{\alpha}$-folded state. The E_2 alloy transition splits into two X_{5v}-split components, while the E_0' transition splits into two Γ_{15v}-split components.

Having established the mapping between the alloy and superlattice E_1, E_2, and E_0' transitions, we next evaluate whether ordering raises or lowers the corresponding transition energies. For this purpose, we use single space-group notations. The direction of the energy-level shift can be predicted by recognizing that folded states with the same symmetry repel each other so that the lowest (highest) moves to yet lower (higher) energies. The main repelling states are as follows.

(a) At $\bar{\Gamma}$, the $\bar{\Gamma}_{3v}(\Gamma_{15v})$ and $\bar{\Gamma}_{3v}(L_{3v})$ states repel each other, raising the energy of $\bar{\Gamma}_{3v}(\Gamma_{15v})$ and lowering the energy of $\bar{\Gamma}_{3v}(L_{3v})$. Similarly, the $\bar{\Gamma}_{1c}(\Gamma_{1c})$ and $\bar{\Gamma}_{1c}(L_{1c})$ states also repel each other, lowering the energy of $\bar{\Gamma}_{1c}(\Gamma_{1c})$ and raising the energy of $\bar{\Gamma}_{1c}(L_{1c})$. These repulsions lower the E_0 transition energy relative to the disordered zinc-blende alloy. (A more detailed discussion on the E_0 transition can be found elsewhere.[3,4]) A similar level repulsion exists between the $\bar{\Gamma}_{3c}(\Gamma_{15c})$ and $\bar{\Gamma}_{3c}(L_{3c})$ states, lowering the energy of $\bar{\Gamma}_{3c}(\Gamma_{15c})$ and raising the energy of $\bar{\Gamma}_{3c}(L_{3c})$. This is expected to reduce the E_0' transition energy [Eq. (3)].

(b) Along the $\bar{\alpha}$ line (Fig. 2), strong repulsions exist between the two folded $\bar{\alpha}_{3v}(\Lambda_{3v})$ states and the two $\bar{\alpha}_{1c}(\Lambda_{1c})$ states. These repulsions move the energy of the lower branch down and the energy of the higher branch up. The repulsion could be very large at the $\bar{Z}$ point, where the corresponding folded zinc-blende states are degenerate. This repulsion can significantly change the E_1 transition along this line.

(c) At the $\bar{D}$ point, the valence-band repulsion occurs between folded $\bar{D}_v(X_{5v})$ and $\bar{D}_v(L_{3v})$ states having the same symmetry (Figs. 3 and 4). This repulsion is expected to raise the energy of $\bar{D}_v(L_{3v})$ and to lower the energy of $\bar{D}_v(X_{5v})$. In the conduction band the three $\bar{D}_{1c}(L_{1c})$, $\bar{D}_{1c}(X_{1c})$, and $\bar{D}_{1c}(X_{3c})$ states can couple to each other. The coupling between these states is expected to lower the energy of the $\bar{D}_{1c}(L_{1c})$ state and raise the energy of the $\bar{D}_{1c}(X_{3c})$ state. Near $\bar{D}$ the repulsions along the $\bar{\beta}$ line (Fig. 3) are similar to that at $\bar{D}$. These repulsions are expected to lower the $E_1(\bar{\beta})$ transition energies [Eq. (1)] and raise the E_2 transition energies [Eq. (2)]. The repulsion along the $\bar{\gamma}$ line (Fig. 4) near $\bar{D}$ is expected to be strong since the two folded Γ_{1c}-X_{1c} and L_{1c}-L_{1c}^* cross each other. This could have large effects on the E_2 transition.

III. BAND-STRUCTURE CALCULATION

Quantitative evaluations of the degree of level shifts require band-structure calculations. Using the first-principles linear augmented plane-wave (LAPW) method[14] within the local-density-functional formalism (LDA),[15] we have calculated the energy-level shift of fully ordered $Ga_{0.5}In_{9.5}P$. Spin-orbit coupling is included. Energies of spin-split states (due to the lack of inversion symmetry in the system) along the low-symmetry lines ($\bar{\beta}$ and $\bar{\gamma}$) are averaged. The LDA errors in the band gap are corrected approximately using the method of Ref. 2. Since we are primarily concerned with the relative energy differences of the same zinc-blende-derived states with different degrees of ordering, we expect that the LDA error will largely cancel in this comparison. The E_0 transition energy for the random alloy is obtained by averaging over the E_0 transitions of more than 20 configurations. For the random common-anion $Ga_{0.5}In_{0.5}P$ system we find that this E_0 energy is only 0.04 eV smaller than the average of the E_0 transition energies of GaP and InP deformed to the same lattice constant of the disordered alloy. Thus, for the other transitions we simply take the average values of GaP and InP evaluated at the alloy lattice constant. The uncertainty due to this approximation is expected to be less than 0.05 eV. Our calculations are

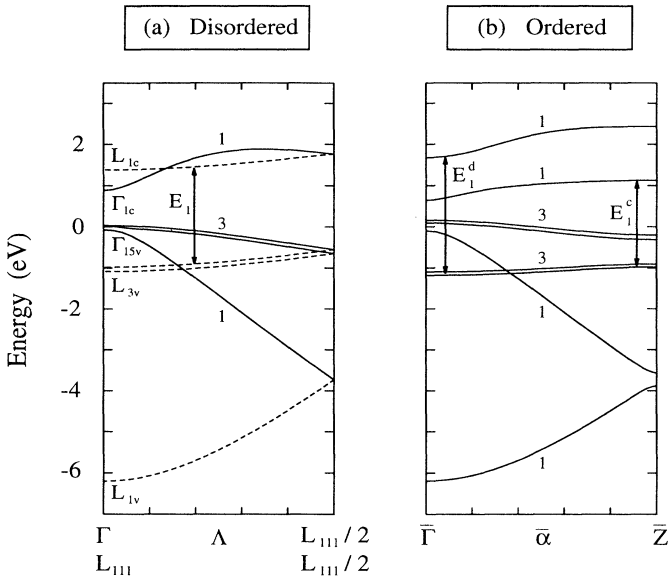

FIG. 2. Calculated fully relativistic band structure of $Ga_{0.5}In_{0.5}P$ along the $\bar{\alpha}$ line parallel to the ordering direction. (a) For the disordered alloy. The dashed lines are the zinc-blende $L_{111}-L_{111}/2$ states folded to the smaller CuPt Brillouin zone. (b) For the fully ordered alloy. The LDA error is not corrected in the plot. The symmetry labels for the lines are single space-group notations. The positions of the direct E_1 transitions are indicated in the figure.

summarized in Table I, and show the following results.

(i) The calculated crystal-field splittings for fully ordered $Ga_{0.5}In_{0.5}P$ [0.20 eV at $\bar{\Gamma}_v(\Gamma_{15v})$, 0.10 eV at $\bar{D}_v(L_{3v})$, -0.08 eV at $\bar{D}_v(X_{5v})$, and -0.12 eV at $\bar{\Gamma}_c(\Gamma_{15c})$] are found to be mostly due to the bond-length relaxations. If one neglects bond relaxation (i.e., assuming equal Ga-P and In-P bond lengths), the splittings are much smaller (<0.03 eV). Hence, level repulsions due to the chemical piece of the coupling potential are small for these pure p states.[16] This is so since for this common-anion alloy the atomic orbital energy disparity between Ga $4p$ and In $5p$ is small (~ 0.04 eV).

(ii) The level repulsions due to the chemical piece of the coupling potential in the conduction bands are large for states with large cation s characters, since the atomic energy disparity between Ga $4s$ and In $5s$ is large (~ 0.69 eV). Bond relaxation further enhances the repulsion.

(iii) At the $\bar{\Gamma}$ point the largest repulsion is between $\bar{\Gamma}_{1c}(\Gamma_{1c})$ and $\bar{\Gamma}_{1c}(L_{1c})$. This repulsion, together with the crystal-field splitting at the top of valence band, lowers the E_0 $[\bar{\Gamma}_{4v,5v}(\Gamma_{15v}) \leftrightarrow \bar{\Gamma}_{6c}(\Gamma_{1c})]$ transition energy[3,4] by 0.32 eV.

(iv) Ordering leads to new, pseudodirect transitions between $\bar{\Gamma}_v(\Gamma_{15v})$ and $\bar{\Gamma}_c(L_{1c})$ states. These transitions are dipole forbidden in an ideal zinc-blende disordered alloy, but are weakly allowed in a CuPt-ordered superlattice. Since $\bar{\Gamma}_{1c}(L_{1c})$ is repelled upwards, the $E_{\Gamma L}[\bar{\Gamma}_v(\Gamma_{15v}) \leftrightarrow \bar{\Gamma}_c(L_{1c})]$ transition energies in the or-

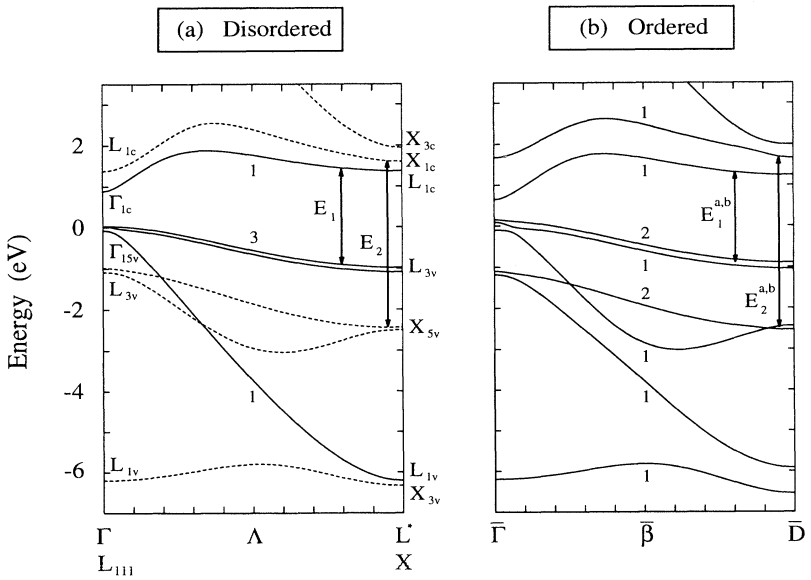

FIG. 3. Calculated fully relativistic band structure of $Ga_{0.5}In_{0.5}P$ along the $\bar{\beta}$ line. (a) For the disordered alloy. The dashed lines are the zinc-blende $L_{111}-X$ states folded to the smaller CuPt Brillouin zone. (b) For the fully ordered alloy. The LDA error is not corrected in the plot. The symmetry labels for the lines are single space-group notations. The positions of the direct E_1 and E_2 transitions are indicated in the figure.

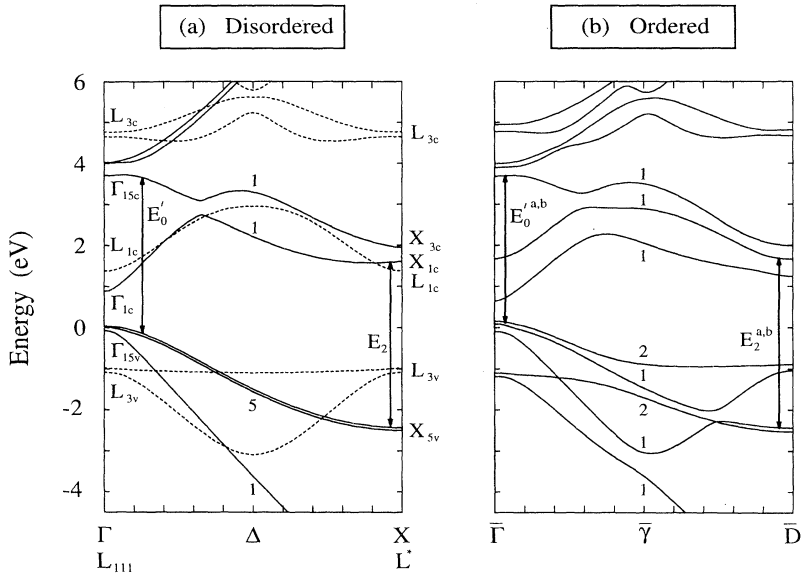

FIG. 4. Calculated fully relativistic band structure of $Ga_{0.5}In_{0.5}P$ along the $\bar{\gamma}$ line. (a) For the disordered alloy. The dashed lines are the zinc-blende $L_{111}-L^*$ states folded to the smaller CuPt Brillouin zone. (b) For the fully ordered alloy. The LDA error is not corrected in the plot. The symmetry labels for the lines are single space-group notations. The positions of the direct E_2 and E_0' transitions are indicated in the figure.

TABLE I. Predicted direct E_0, E_1, E_2, and E_0' transition energies and some pseudodirect transition energies in partially ordered $Ga_{0.5}In_{0.5}P$ as functions of ordering parameter η. The symmetry point label with an overbar denotes states in the CuPt Brillouin zone (Fig. 1), while the symbol in parentheses is the parent zinc-blende states. In the disordered alloy $E_1^a(\eta=0)=E_1+\Delta_L$, $E_2^b(\eta=0)=E_2+\Delta_X$, and $E_{\Gamma L}^c(\eta=0)=E_{\Gamma L}(0)+\Delta_0$, where Δ_L, Δ_X, and Δ_0 (0.09, 0.07, and 0.10 eV, respectively) are spin-orbit splittings at L, X, and Γ, respectively. The energy-level differences $E_{\Gamma L}(0)$, $E_{XL}(0)$, and $E_{LX}(0)$ for the disordered alloy are not accurately determined experimentally. They are estimated (Refs. 10, 13, and 17) to be about 2.2, 5.0, and 3.4 eV, respectively. The + sign in the last column means that ordering raises the energy, while the − sign means that it lowers the energy relative to the disordered alloy. The pseudodirect transitions are dipole forbidden in the disordered alloy. Energies are in eV.

Designation / Direct transitions	Name	Energy
$\bar{\Gamma}_{4v,5v}(\Gamma_{15v})\leftrightarrow\bar{\Gamma}_{6c}(\Gamma_{1c})$	$E_0(\eta)$	$E_0(0)-0.32\eta^2$
$\bar{\beta}_{3v}(\Lambda_{3v})\leftrightarrow\bar{\beta}_{3c}(\Lambda_{1c})$	$E_1^a(\eta)$	$[E_1(0)+\Delta_L]-0.16\eta^2$
$\bar{\beta}_{4v}(\Lambda_{3v})\leftrightarrow\bar{\beta}_{3c}(\Lambda_{1c})$	$E_1^b(\eta)$	$E_1(0)-0.22\eta^2$
$\bar{\alpha}_{4v,5v}(\Lambda_{3v})\leftrightarrow\bar{\alpha}_{6c}(\Lambda_{1c})$	$E_1^c(\eta)$	$E_1(0)-0.30\eta^2$
$\bar{\alpha}_{4v,5v}(L_{3v})\leftrightarrow\bar{\alpha}_{6c}(L_{1c})$	$E_1^d(\eta)$	$E_1(0)+0.41\eta^2$
$\bar{\gamma}_{3v}(X_{5v})\leftrightarrow\bar{\gamma}_{3c}(X_{1c})$	$E_2^a(\eta)$	$E_2(0)+0.05\eta^2$
$\bar{\gamma}_{4v}(X_{5v})\leftrightarrow\bar{\gamma}_{3c}(X_{1c})$	$E_2^b(\eta)$	$[E_2(0)+\Delta_X]+0.08\eta^2$
$\bar{\Gamma}_{4v,5v}(\Gamma_{15v})\leftrightarrow\bar{\Gamma}_{6c}(\Gamma_{15c})$	$E_0'^a(\eta)$	$E_0'(0)-0.15\eta^2$
$\bar{\Gamma}_{6v}(\Gamma_{15v})\leftrightarrow\bar{\Gamma}_{6c}(\Gamma_{15c})$	$E_0'^b(\eta)$	$E_0'(0)-0.09\eta^2$
Pseudodirect transitions		
$\bar{\Gamma}_{4v,5v}(\Gamma_{15v})\leftrightarrow\bar{\Gamma}_{6c}(L_{1c})$	$E_{\Gamma L}^a(\eta)$	$E_{\Gamma L}(0)+0.17\eta^2$
$\bar{\Gamma}_{6v}(\Gamma_{15v})\leftrightarrow\bar{\Gamma}_{6c}(L_{1c})$	$E_{\Gamma L}^b(\eta)$	$E_{\Gamma L}(0)+0.23\eta^2$
$\bar{\Gamma}_{6v}^{SO}(\Gamma_{15v})\leftrightarrow\bar{\Gamma}_{6c}(L_{1c})$	$E_{\Gamma L}^c(\eta)$	$[E_{\Gamma L}(0)+\Delta_0]+0.33\eta^2$
$\bar{D}_{3v}(X_{5v})\leftrightarrow\bar{D}_{3c}(L_{1c})$	$E_{XL}(\eta)$	$E_{XL}(0)-0.14\eta^2$
$\bar{D}_{4v}(L_{3v})\leftrightarrow\bar{D}_{3c}(X_{1c})$	$E_{LX}(\eta)$	$E_{LX}(0)-0.04\eta^2$

dered superlattice are above the corresponding $\Gamma_{15v}-L_{1c}$ energy difference in the disordered alloy. Taking into account the crystal-field splitting and the spin-orbit splitting at the top of valence band, we denote the three $E_{\Gamma L}$ transitions as

$$E_{\Gamma L}^a[\bar{\Gamma}_{4v,5v}(\Gamma_{15v})\leftrightarrow\bar{\Gamma}_{6c}(L_{1c})]\ ,$$
$$E_{\Gamma L}^b[\bar{\Gamma}_{6v}(\Gamma_{15v})\leftrightarrow\bar{\Gamma}_{6c}(L_{1c})]\ , \quad (4)$$
$$E_{\Gamma L}^c[\bar{\Gamma}_{6v}^{SO}(\Gamma_{15v})\leftrightarrow\bar{\Gamma}_{6c}(L_{1c})]\ .$$

Assuming[17] that for disordered $Ga_{0.5}In_{0.5}P$ alloy the energy difference $E_{\Gamma L}$ between Γ_{8v} and L_{6c} is 2.20 eV, we find that in the fully ordered superlattice the pseudodirect transitions $E_{\Gamma L}^a$ occur at 2.37 eV, the transition $E_{\Gamma L}^b$ from the crystal field split-off band[4] at 2.43 eV, and $E_{\Gamma L}^c$ from the spin-orbit split-off band at 2.63 eV.

(v) Relative to the E_0' transition in the disordered alloy, the $E_0'^a$ transition energy in fully ordered $Ga_{0.5}In_{0.5}P$ [Fig. 4(b)] is lowered by 0.15 eV, while the $E_0'^b$ transition energy is lowered by 0.09 eV. These energy lowerings are due mainly to crystal-field splitting in the two corresponding states.

(vi) For the $\bar{D}_{1c}$ states (Figs. 3 and 4), we find strong repulsion only between the L_{1c}- and X_{3c}-derived states, having large cation s character. The energy of the X_{1c}-derived state is found to be essentially unaffected (to within 0.02 eV) by the ordering, since X_{1c} is an anion s and cation p state. We find that, relative to the disordered alloy, the E_2^a transition energy in fully ordered $Ga_{0.5}In_{0.5}P$ [Figs. 3(b) and 4(b)] is increased by 0.05 eV, while the E_2^b transition energy is increased by 0.15 eV (0.08 eV relative to $E_2+\Delta_X$, where $\Delta_X=0.07$ eV is the calculated spin-orbit splitting of the X_{5v} state). Ordering also leads to a weak E_2-like transition $E_{XL}[\bar{D}_{3v}(X_{5v})\leftrightarrow\bar{D}_{3c}(L_{1c})]$ in a region near $\bar{D}$ [Figs. 3(b)

and 4(b)]. For the fully ordered superlattice, this E_{XL} transition is 0.14 eV lower than the $X_{7v}-L_{6c}$ energy difference in the disordered alloy.

(vii) The E_1 transition in the ordered superlattice splits into E_1^a and E_1^b components on the $\bar{\beta}$ lines (Fig. 3) and the E_1^c component on the $\bar{\alpha}$ line along the ordering direction (Fig. 2). We find that, relative to the disordered alloy, the E_1^a transition energies of the fully ordered superlattice are lowered by 0.07 eV (0.16 eV relative to $E_1+\Delta_L$, where $\Delta_L=0.09$ eV is the calculated spin-orbit splitting of the L_{3v} state), and the E_1^b transition energy is lowered by 0.22 eV. There is also the weak, zinc-blende-forbidden E_1-like transition $E_{LX}[\bar{D}_{4v}(L_{3v})\leftrightarrow\bar{D}_{3c}(X_{1c})]$ in a region near $\bar{D}$ [Figs. 3(b) and 4(b)], which is 0.04 eV lower than the $L_{4v,5v}-X_{6c}$ energy difference in the disordered alloy. The shape of the band structure along the ordering direction ($\bar{\alpha}$) changed drastically due to the strong repulsion between the coupling states near the band edge. Inspection of the band structure of the fully ordered $Ga_{0.5}In_{0.5}P$ superlattice [Fig. 2(b)] shows that the dominant E_1^c transition occurs between the lower branch of $\bar{\alpha}_{4,5v}(\Lambda_{3v})$ and the lower branch of $\bar{\alpha}_{6c}(\Lambda_{1c})$ near $\bar{Z}$. The wave functions for these two branches are more localized on the GaP sublattice. The other two complementary branches are more localized on the InP sublattice. Relative to the disordered alloy, this dominant E_1^c transition is 0.30 eV lower than the E_1 transition in the disordered alloy. There are also other weak E_1-type transitions along this direction. For example, the E_1^d transition comes from states near $\bar{\Gamma}$ between the lower branch of $\bar{\alpha}_{4,5v}(\Lambda_{3v})$ and the higher branch of $\bar{\alpha}_{6c}(\Lambda_{1c})$ [Fig. 2(b)]. It has a transition energy 0.41 eV higher than the E_1 transition in the disordered alloy. This transition is weak because it has small joint density of state, and the pairs of the transition states are localized on different sublattice.

(viii) For partially ordered samples ($0\le\eta\le1$, where η is the ordering parameter) we can use the theory of Ref. 3, which predicts approximately that the dependence of transition energies on ordering is given by

$$E_i(\eta)=E_i(0)+[E_i(1)-E_i(0)]\eta^2 , \tag{5}$$

where $E_i(1)$ and $E_i(0)$ are the transition energies of fully ordered and perfectly disordered alloys, respectively. A more accurate transition-energy dependence on the ordering parameter requires explicit treatment of coupling between crystal-field splitting and the spin-orbit splitting.[3,4] For all transitions discussed above, the predicted transition energies as function of ordering parameter η are given in Table I.

(ix) Since all the transition energies are approximately quadratic functions[3] of η, the ratio

$$\xi_{ij}(\eta)=[E_i(\eta)-E_i(0)]/[E_j(\eta)-E_j(0)] \tag{6}$$

between the ordering-induced changes of transitions i and j is approximately a constant. For example, the slopes ξ of E_1^a, E_1^b, E_1^c, and E_1^d versus E_0 are calculated to be 0.50, 0.69, 0.94, and -1.28, respectively. Note that the E_1^c and E_1^d transitions are nonzero only for light polarized perpendicular to the ordering direction, while E_1^a and E_1^b are allowed for both parallel and perpendicular polarizations. Their intensities depend on ratio between the crystal-field splitting and the spin-orbit splitting.[12,18]

The E_1 energy lowering in ordered $Ga_{0.5}In_{0.5}P$ has been observed before.[11] Recently, Alsina *et al.*[12] measured the energy shift of the E_1 transition in $Ga_{0.5}In_{0.5}P$ as a function of the CuPt ordering parameter (derived from the E_0 band-gap reduction[3]) and light polarization. They found two transitions, both decreasing in energy when the degree η of ordering increases from zero. The measured slopes [ξ of Eq. (6)] of $E_1^{\parallel}$ and $E_1^{\perp}$ versus E_0 are 0.63 and 1.11, respectively. These results are in good agreement with our calculated values if we assign $E_1^{\parallel}$ as a mixture of E_1^a and E_1^b, and assign $E_1^{\perp}$ as E_1^c. Similar conclusions are reached by Alsina *et al.*[12]

The position of the X_{1c}-derived states in the ordered superlattice was the subject of a recent experiment by Uchida *et al.*,[13] who performed pressure-dependent photoluminescence in both ordered and disordered $Ga_{0.5}In_{0.5}P$. By linearly extrapolating from high-pressure data (beyond the direct-indirect transition) they concluded that at zero pressure the energy of the X_{1c}-derived state in the ordered alloy is lowered by the same amount as the $\bar{\Gamma}_{1c}(\Gamma_{1c})$ state. Since the lowering of the X_{1c}-derived state is not expected in CuPt ordering (having L but not X folding into $\bar{\Gamma}$), they suggest that the lowering of the X_{1c} energy is a fingerprint of the presence of a non-CuPt ordering (e.g., the $Y2$ structure) in the sample. This conclusion is not supported by the present calcula-

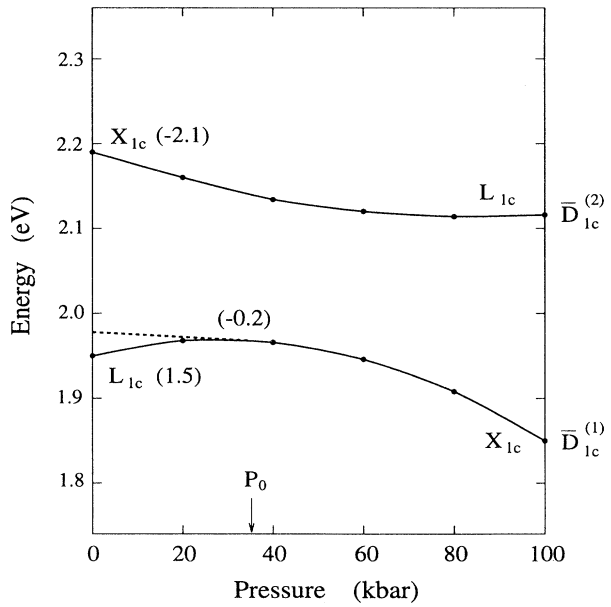

FIG. 5. Calculated pressure dependence of the energy levels of $\bar{D}_{1c}^{(1)}$ and $\bar{D}_{1c}^{(2)}$ states of the fully ordered $Ga_{0.5}In_{0.5}P$ structure. The numbers in parentheses are the calculated deformation potentials (in meV/kbar) at zero pressure and at $P_0=35$ kbar. The dashed line indicates linear extrapolation to zero pressure. Note the anticrossing and the ensuing changes of wave-function character with pressure.

tion, since the application of linear extrapolation at low pressure is inappropriate when avoided crossing exists: The folded $\bar{D}_{1c}(X_{1c})$ and $\bar{D}_{1c}(L_{1c})$ states have the same symmetry. The mixing of the two states is small at zero pressure. However, as pressure is applied, the difference in their deformation potentials (positive for L_{1c}, negative for X_{1c}) causes the $\bar{D}_{1c}(L_{1c})$ state to move up in energy while the $\bar{D}_{1c}(X_{1c})$ state moves down in energy. When the two $\bar{D}_{1c}$ states come close to each other, anticrossing causes a large wave-function mixing between them. Hence, linear extrapolating of the high-pressure data will lead to a zero-pressure energy much lower than the energy of the actual $\bar{D}_{1c}(X_{1c})$ state. To test this point quantitatively, we used the LAPW method to calculate the energy levels of $\bar{D}_{1c}^{(1)}$ and $\bar{D}_{1c}^{(2)}$ as functions of pressure (Fig. 5). At zero pressure, $\bar{D}_{1c}^{(1)}$ is a zinc-blende L_{1c}-derived state (with some X_{3c} character). The calculated deformation potential for the fully ordered sample is $+1.5$ meV/kbar. The $\bar{D}_{1c}^{(2)}$ state is a pure X_{1c} state with a negative deformation potential of -2.1 meV/kbar. As the pressure increases, anticrossing causes the two $\bar{D}_{1c}$ states to change character: $\bar{D}_{1c}^{(1)}$ becomes more X_{1c} like, while $\bar{D}_{1c}^{(2)}$ becomes more L_{1c} like. At $P_0=35$ kbar (the observed direct-indirect crossover pressure[13]), the calculated deformation potential is -0.2 meV/kbar, close to the experimental value[13] of -0.5 meV/kbar. Using this slope, linear extrapolation to zero pressure (shown as the dashed line in Fig. 5) gives an energy of 1.97 eV, i.e., 0.22 eV lower than the actual energy of the $\bar{D}_{1c}(X_{1c})$ state (at about 2.19 eV in Fig. 5). This extrapolated state at 1.97 eV should not be confused with the actual X_{1c} state at 2.19 eV. The latter, as we said above, is practically unshifted relative to the X_{1c} state in the disorderd alloy. This result is consistent with our argument above. Thus, the experimental data[13] cannot be used to support the existence of non-CuPt ($Y2$) ordering in the experimental sample. We see from Fig. 5 that if the experiment[13] was extended to higher pressure (>100 kbar), linear extrapolation would be more accurate.

IV. SUMMARY

We have performed a quantitative theoretical study of the ordering-induced effects on high-energy E_1, E_2, and E_0' transitions using symmetry arguments and first-principles band-structure calculations. We find that upon ordering these transitions are altered dramatically—some states shift up in energy, some shift down, and new ordering-induced transitions, absent in the disordered phase now become allowed. Experimental observation of these changes could serve as new fingerprints of ordering. Our results compare well with recent experimental data. We have also studied the positions of the X_{1c}- and L_{1c}-derived states in the ordered superlattice, and found that the superlattice is unchanged relative to the disordered alloy at zero pressure. The experimentally observed "X_{1c}-like" state at higher pressure is identified as a mixture of the folded L_{1c} and X_{1c} states.

ACKNOWLEDGMENTS

We thank Dr. Hosun Lee and Dr. Sam Luo for useful discussions, and Dr. F. Alsina for providing us Ref. 12 before its publication and for very helpful comments regarding the E_1 transition in the ordered superlattice. This work was supported in part by U.S. Department of Energy, Grant No. DE-AC02-83-CH10093.

[1]For a recent review on spontaneous ordering in semiconductor alloys, see A. Zunger and S. Mahajan, in *Handbook of Semiconductors*, 2nd ed., edited by S. Mahajan (Elsevier, Amsterdam, 1994), Vol. 3, p. 1399, and references therein.

[2]S.-H. Wei and A. Zunger, Phys. Rev. B **39**, 3279 (1989).

[3]S.-H. Wei, D. B. Laks, and A. Zunger, Appl. Phys. Lett. **62**, 1937 (1993).

[4]S.-H. Wei and A. Zunger, Appl. Phys. Lett. **64**, 757 (1994); **64**, 1676 (1994); Phys. Rev. B **49**, 14 337 (1994).

[5]T. Kuromot and N. Hamada, Phys. Rev. B **40**, 3889 (1989).

[6]T. Nishino, J. Cryst. Growth **98**, 44 (1989).

[7]T. Kanata, M. Nishimoto, H. Nakayama, and T. Nishino, Phys. Rev. B **45**, 6637 (1992).

[8]T. Kanata, M. Nishimoto, H. Nakayama, and T. Nishino, Appl. Phys. Lett. **63**, 26 (1993).

[9]R. G. Alonso, A. Mascarenhas, G. S. Horner, K. A. Bertness, S. R. Kurtz, and J. M. Olson, Phys. Rev. B **48**, 11 833 (1993).

[10]C. Alibert, G. Bordure, A. Laugier, and J. Chevallier, Phys. Rev. B **6**, 1301 (1972).

[11]T. Nishino, Y. Inoue, Y. Hamakawa, M. Kondow, and S. Minagawa, Appl. Phys. Lett. **53**, 583 (1988).

[12]F. Alsina, M. Garriga, M. I. Alonso, J. Pascual, J. Camassel, and R. W. Glew, in *Proceedings of the 22nd International Conference on the Physics of Semiconductors, Vancouver, Canada*, edited by D. J. Lockwood (World Scientific, Singapore, 1994), p. 253.

[13]K. Uchida, P. Y. Yu, N. Noto, and E. R. Weber, Appl. Phys. Lett. **64**, 2858 (1994).

[14]S.-H. Wei and H. Krakauer, Phys. Rev. Lett. **55**, 1200 (1985), and references therein.

[15]D. M. Ceperly and B. J. Alder, Phys. Rev. Lett. **45**, 566 (1980); J. P. Perdew and A. Zunger, Phys. Rev. B **23**, 5048 (1981).

[16]Here we neglect small p-d mixing in the wave function for this system.

[17]H. Lee, Ph.D. thesis, University of Illinois at Urbana-Champaign, 1993.

[18]F. H. Pollak and G. W. Rubloff, Phys. Rev. Lett. **29**, 789 (1972); F. H. Pollak, Surf. Sci. **37**, 863 (1973).